

Original Article

Metformin induces M2 polarization via AMPK/PGC-1 α /PPAR- γ pathway to improve peripheral nerve regeneration

Zekun Zhou^{1*}, Gaojie Luo^{1*}, Cheng Li¹, Peiyao Zhang¹, Wei Chen¹, Xiaoxiao Li², Juyu Tang^{1*}, Liming Qing^{1*}

¹Department of Orthopedics, Hand and Microsurgery, Xiangya Hospital of Central South University, Changsha, Hunan, China; ²Department of Pathology, Changsha Medical University, Changsha, Hunan, China. *Equal contributors and co-first authors.

Received March 26, 2023; Accepted May 4, 2023; Epub May 15, 2023; Published May 30, 2023

Abstract: Objectives: Investigating the effect of metformin on peripheral nerve regeneration and the molecular mechanism. Methods: In this study, a rat model of sciatic nerve injury and an inflammatory bone marrow-derived macrophage (BMDM) cell model were established. We assessed the sensory and motor function of the hind limbs four weeks after sciatic nerve injury, immunofluorescence was used to detect axonal regeneration and myelin formation, as well as local macrophage subtypes. We investigated the polarizing effect of metformin on inflammatory macrophages, and western blotting was applied to detect the molecular mechanisms behind it. Results: Metformin treatment accelerated functional recovery, axon regeneration and remyelination, and promoted M2 macrophage polarization. *In vivo*, metformin transformed pro-inflammatory macrophages into pro-regeneration M2 macrophages. Protein expression levels of phosphorylated AMP-activated protein kinase (p-AMPK), proliferator-activated receptor- γ co-activator 1 α (PGC-1 α), and peroxisome proliferator-activated receptor- γ (PPAR- γ) increased upon metformin treatment. Moreover, inhibition of AMPK abolished the effects of metformin treatment on M2 polarization. Conclusion: Metformin promoted M2 macrophage polarization by activating the AMPK/PGC-1 α /PPAR- γ signaling axis, thereby promoting peripheral nerve regeneration.

Keywords: Metformin, peripheral nerve regeneration, macrophage polarization, AMPK/PGC-1 α /PPAR- γ signaling axis

Introduction

Peripheral nerve injury (PNI) remains a significant clinical challenge and public health burden worldwide. Although the peripheral nervous system has the potential for self-healing, the capacity for regeneration is limited [1]. Moreover, existing treatments for PNI are sub-optimal and often result in poor functional recovery. Recent evidence demonstrated that macrophages play a key role in the peripheral nerve regeneration process. Macrophages can be classified into the “classically activated” M1 phenotype, which is pro-inflammatory, and the “alternatively activated” M2 phenotype, which is anti-inflammatory [2, 3]. It has been shown that M2 macrophages secrete a variety of pro-axonal regeneration factors, including growth factors, cytokines, chemokines, and extracel-

lular matrix (ECM), to inhibit inflammation, regulate fibroblast regeneration, and promote angiogenesis to synergistically regulate peripheral nerve regeneration [4-6]. In addition, non-functional or dysfunctional M2 macrophages inhibit axon regeneration and injure normal axons during the nerve regeneration process [7]. Therefore, orderly and timely M2 polarization is critical for peripheral nerve regeneration.

Metformin, a widely used hypoglycemic agent, is currently one of the most common medications for type 2 diabetes. Recently, it has been shown that metformin has anti-inflammatory properties [8-10]. Emerging evidence supports the novel hypothesis that metformin regulates immune cell function [11, 12]. Our previous research showed that metformin accelerates M2 macrophage polarization to promote wound

healing [13]. However, the ability of metformin to affect M2 macrophage polarization during peripheral nerve regeneration has not yet been examined. Earlier studies demonstrated that the pleiotropic effects of metformin are associated with activation of AMP-activated protein kinase (AMPK) [14, 15]. In addition, numerous studies have demonstrated that AMPK is involved in the process of nerve regeneration [16-18]. Peroxisome proliferator-activated receptor- γ co-activator 1 α (PGC-1 α) is a downstream target of AMPK that regulates mitochondrial biogenesis and reactive oxygen species synthesis [19, 20]. PGC-1 α is also an important ligand for peroxisome proliferator-activated receptors (PPARs), a class of ligand-activated transcription factors in the nuclear receptor superfamily. Of the various PPARs, PPAR- γ , the major isoform in the PPAR family, is prevalent in neural tissues, including neurons, microglia, and astrocytes [21]. The interaction between PGC-1 α and PPAR- γ is neuroprotective and has positive effects on diseases, such as multiple sclerosis [22, 23], amyotrophic lateral sclerosis [24, 25], Alzheimer's disease [26, 27], and Parkinson's disease [28, 29]. Our previous research also found that metformin has immunomodulatory properties and exerts anti-inflammatory effects by activating the AMPK protein [13]. Recently, emerging studies confirmed that the AMPK/PGC-1 α /PPAR- γ signaling pathway is involved in the anti-inflammatory process and macrophage polarization [30, 31]. However, the role of AMPK/PGC-1 α /PPAR- γ signaling in the immunomodulatory function of metformin needs further clarification. This study aimed to examine the effects of metformin on peripheral nerve regeneration and to elaborate on the related mechanism.

Material and methods

Establishment of a rat model of PNI and drug treatment

The sciatic crushing model was established as described in our previous study. In brief, Sprague-Dawley (SD) rats were chosen and separated into two groups: the control group and the 50 mg/kg metformin group [13]. The rats were anesthetized with 3% pentobarbital sodium (40 mg/kg) via intraperitoneal (IP) injection. Then, a 1.5 cm deep incision was made using sterile hemostatic forceps and tissue

scissors at the posterior-thigh muscle to expose the sciatic nerve. The exposed nerves were clamped with hemostatic forceps for 10 s and then relaxed for 10 s; this procedure was repeated up to three times. Impaired nerves were marked with surgical 10-0 nylon monofilament and were harvested after 4 weeks to evaluate nerve regeneration. After surgery, 50 mg/kg metformin or equal doses of PBS were administered to the rats via IP injection until the endpoint of observation. The rats were housed with free access to water and food in the Animal Care Center of Xiangya Hospital, Central South University (Changsha, Hunan, China). All surgical procedures and other manipulations were administered in compliance with the guidelines of the China Council of Animal Care after obtaining approval from the Central South University Committee on Laboratory Animals.

Assessment of sensory and motor functional recovery

Assessment of sensory and motor functional recovery following PNI was described in our previous study [32]. In brief, after inducing the nerve-crushing injury, sensory recovery was assessed by thermo-sensitivity analysis and the Von-Frey test. First, the rats were moved onto a metal platform with the temperature controlled between 50-55°C. The time taken to observe a nocifensive behavior, such as jumping, stamping, leaning posture, and hind paw withdrawal or licking, was recorded as the latency. Second, the Von-Frey test was conducted with the rats placed on mesh. Specifically, monofilaments of different forces were applied perpendicularly to the plantar surface of the hind paw for 2-5 s. A positive response was defined as hind paw withdrawal, licking, or paw shaking. By setting the mechanical withdrawal threshold as the force of the last von Frey monofilament, the force of monofilaments was increased continuously until reaching a response rate of 40% or more.

To assess recovery of sciatic nerve motor function, the sciatic function index (SFI) and the Basso, Beattie, and Bresnahan (BBB) locomotor rating were evaluated at 0, 1, 3, 7, 14, and 28 d post-operation [33]. During the SFI test, after dipping the hind feet of the rats in ink, the rats were allowed to walk through a tunnel cov-

Metformin in nerve regeneration

ered with paper to record footprints. Then, toe spread (TS), the distance between the first and fifth toe; intermediary toe spread (ITS), the distance between the second and fourth toe; and print length (PL), the distance between the third toe and heel, were evaluated on the injured (E) side (ETS, EITS, and EPL, respectively) and normal (N) side (NTS, NITS, and NPL, respectively). Subsequently, the SFI was computed using the following formula: $SFI = -38.3 \times (EPL-NPL)/NPL + 109.5 \times (ETS-NTS)/NTS + 13.3 \times (EITS-NITS)/NITS - 8.8$ [34]. An independent observer was engaged to determine the BBB Locomotor Rating of the rats in an arena in an open field. Moreover, sciatic nerve function was evaluated through ankle kinematics. For the sagittal plane analysis, the ankle angle, represented as the degree at terminal stance, was measured as the intersection of the line extending from the lateral epicondyle to the lateral malleolus and from the lateral malleolus to the metatarsal head. Further, the muscle weight ratio was measured using the formula: muscle weight ratio = the wet weight of the gastrocnemius muscle on the injured side/the wet weight of the gastrocnemius muscle on the contralateral normal side as described previously [32].

Electrophysiology

Previously, we described the electrophysiological recording protocol for peripheral nerve regeneration [32]. In brief, electrophysiological recordings were conducted at 4 weeks post-operation using a Tucker-Davis Technologies system (TDT, Alachua, FL) with a preamplifier. The stimulating electrodes were fixed 5 mm away from the crushed proximal sciatic nerve of the rats, and the recording electrodes were fixed near the sciatic nerve and 5 mm away from the crushed distal sciatic nerve. After stimulating the sciatic nerve electrically (0.5 mA, stimulation frequency 0.5 Hz, and pulse duration 100 μ s) through the proximal interfascicular electrode, compound motor action potential (CMAP) at the distal interfascicular electrode was recorded. Peak-to-peak amplitude was analyzed using OriginPro 8 software. Data were blinded and assessed by trained technicians.

Retrograde tracing

The retrograde tracing test was performed as described previously [32]. In brief, rats

were injected with 10 μ l of 1,19-dioctadecyl-3,3,39,39-tetramethylindocarbocyanine perchlorate (Dil) into the tibial nerve at 4 weeks post-injury. After allowing retrograde transport for 48 h, the rats were sacrificed by anesthetization and perfused with saline plus 4% (wt) paraformaldehyde. The L4 and L5 dorsal root ganglia (DRG) were harvested and cryo-sectioned into 20 μ m serial cross-sections. Total numbers of Dil-labeled cells were counted in every alternate section by fluorescence microscopy.

Immunofluorescence

Nerve tissues were excised 4 weeks after injury, fixed with 4% paraformaldehyde, and perforated with 0.3% Triton X-100. The tissues were blocked with 5% BSA and then incubated with primary antibodies at 4°C for 8-12 h. The primary antibodies used were anti-NF200 (axon neurofilament marker, 1:1000, Abcam), anti-MBP (myelin marker, 1:1000, Abcam), anti-CD68 (macrophage marker, 1:1000, Abcam), and anti-CD206 (M2 macrophage marker, 1:1000; Abcam). Tissues were then incubated with secondary antibody at room temperature for 90 min. After washing with TBST for 5 min three times, nuclei were stained with DAPI (Invitrogen, Carlsbad, CA) for 15 min. A fluorescent Nikon N2-DMi8 inverted microscope (Nikon, Kobe, Japan) was used to observe the stained tissues. For quantitative analysis, six different fields were assessed randomly for each sample, and the areas which stained positive for NF200, MBP, CD68, CD206, and DAPI were analyzed using Image J software (Media Cybernetics).

Extraction and stimulation of bone-marrow-derived macrophages (BMDMs)

BMDMs were isolated from the femurs and tibias of C57BL/6j mice weighing 22-25 g as previously described [35]. BMDMs were cultured in Iscove's modified Dulbecco's medium (IMEM; Gibco, USA) with 1% penicillin-streptomycin (NCM Biotech, Suzhou), 10% fetal bovine serum (FBS; New Zealand, USA), and 20 ng/ml M-CSF (Proteinates, USA) for 7 d and then seeded into 6-well plates. On day 8, the cells were treated with 100 ng/ml lipopolysaccharide (LPS, Sigma, USA) for 6 h [13]. Then, BMDMs were divided into three groups: (1) the control group (treated with PBS), (2) the metformin group

Metformin in nerve regeneration

(treated with 2 mM metformin), and (3) the compound C group (treated with 2 mM metformin and 10 μ M compound C) [13]. After 24 h of treatment, cells were collected for subsequent testing.

Cell viability

The CCK-8 kit (NCM Biotech, #C6030) was used to assess cell viability in accordance with the manufacturer's instructions. Specifically, BMDMs were seeded into 96-well plates at a density of 5×10^3 cells/well. Once the cells appeared to be adhered, varying concentrations of metformin (0.5, 1, 2, 4, 8, and 16 mmol/L) were added and the cells were then incubated for 24 or 48 h. Then, 10 μ l of CCK-8 solution was added to each well and the cells were further incubated at 37°C for 3 h. The absorbance of each well was measured at 450 nm using a microplate reader (Thermo Fisher Scientific). The cell viability was calculated using the following equation: Cell viability = ((Absorbance value of metformin group)/(Absorbance value of control group)) * 100%.

Flow cytometry

BMDMs were trypsinized and resuspended in pre-chilled PBS solution. Anti-mouse F4/80-BV421 (BD Biosciences, USA) was used to determine the total macrophage count, anti-mouse CD86-APC (BD Biosciences, USA) was used to determine the M1 macrophage count, and anti-mouse CD206-AF488 (BioLegend, USA) was used to determine the M2 macrophage count. Next, $1-10 \times 10^5$ BMDMs were incubated with antibodies for 30 min on ice and sorted by flow cytometry (Verse, BD Bioscience). The subpopulations of macrophages were analyzed using Flow Jo (Trestar software, Ashland, OR, USA).

Real-time quantitative PCR

Total RNA from BMDMs was extracted with Trizol Reagent (Invitrogen, USA). Synthesis of cDNA was performed according to the manufacturer's protocols (Vazyme, Nanjing, China). The real-time qPCR reaction was performed using a SYBR-Green RT-PCR kit (Vazyme, Nanjing, China). GAPDH was used as the reference, and RNA expression was quantified using the $2^{-\Delta\Delta CT}$ technique. The primer sequences were obtained from NCBI and synthesized by Tsing Ke Biotech as follows: inducible nitric

oxide synthase (iNOS), 5'-GTTCTCAGCCCAACA-ATACAAGA-3' (forward) and 5'-GTGGACGGGTCGATGTACAC-3' (reverse); tumor necrosis factor (TNF- α), 5'-CCCTCACACTCAGATCATCTTCT-3' (forward) and 5'-GCTACGACGTGGGCTACAG-3' (reverse); interleukin-1 β (IL-1 β), 5'-GCAACTGTTCCTGAACTCAACT-3' (forward) and 5'-ATCTTTGGGGTCCGTCAACT-3' (reverse); arginase-1 (Arg-1), 5'-CTCCAAGCCAAAGTCCTTAGAG-3' (forward) and 5'-AGGAGCTGTCATTAGGGACATC-3' (reverse); interleukin-10 (IL-10), 5'-CTTACTGACTGGCATGAGGATCA-3' (forward) and 5'-GCAGCTCTAGGAGCATGTGG-3' (reverse); chitinase 3-like 3 (Ym-1), 5'-CAGGTCTGGCAATTCTTCTGAA-3' (forward) and 5'-GTCTTGCTCATGTGTGTAAGTGA-3' (reverse).

Western blot

Separation of protein extracts from BMDMs (30 μ g) was performed by SDS-PAGE. The separated proteins were transferred onto PVDF membranes. The membranes were blocked with non-fat milk dissolved in TBS with 0.1% Tween 20 at room temperature for 2 h. The membranes were then incubated with primary antibodies against AMPK- α -1 (1:2500, Abcam), Phospho-AMPK- α -1 (Thr183) + Phospho-AMPK- α -2 (T172) (1:5000, Abcam), PGC-1 α (1:1000, Abcam), PPAR- γ (1:1000, Abcam), and GAPDH (1:1000, Abclonal) at 4°C overnight. The membranes were washed with TBST for 5 min three times and then incubated with HRP-conjugated secondary antibody (Abclonal, USA) for 2 h. Bands were detected using the ChemiDoc XRS+ Imaging system (Bio-Rad). Bands were quantified using Imaging Lab (Bio-Rad, United States).

Statistical analysis

Statistical analyses were conducted using GraphPad Prism 8.0 Software (La Jolla, CA, USA), and data were presented as mean \pm SD. The student's t-test was utilized to compare two sets of data. The one-way analysis of variance (ANOVA) and Dunnett's post hoc test were utilized to compare multiple groups. $P < 0.05$ represented statistical significance.

Results

Metformin improved functional recovery after PNI

We investigated motor and sensory functions to evaluate the functional recovery after PNI.

Metformin in nerve regeneration

Specifically, the SFI, the BBB score, ankle angle, and wet weight mass ratio of the gastrocnemius muscle were measured at 4 weeks post-operation to assess motor function recovery. The SFI and BBB scores were higher in the metformin group than in the control group ($P < 0.01$, **Figure 1A** and **1B**). In addition, the ankle angle and the wet weight mass ratio of the gastrocnemius muscle were both higher in the metformin group than in the control group ($P < 0.01$, **Figure 1C** and **1D**). Further, the threshold required for mechanical stimulation was lower in the metformin group than in the control group and the latency period under heat stimulation was shorter for the metformin group than the control group ($P < 0.01$, **Figure 1E** and **1F**). These results suggest that metformin treatment effectively improved functional recovery of the sciatic nerve after injury.

Previous studies demonstrated that improved nerve regeneration was accompanied by electrophysiological improvements, such as increased CMAP. Therefore, to examine the effect of metformin on PNI, CMAP was measured at 2 and 4 weeks post-operation. The peak amplitude of CMAP was higher in the metformin group than in the control group at 4 weeks ($P < 0.01$), but no significant difference was observed at 2 weeks (**Figure 1G** and **1H**). These data indicate that the metformin treatment group achieved significant electrophysiological recovery after PNI. Taken together, metformin treatment improved functional recovery of the hind limb following PNI.

Metformin promoted axonal regeneration and remyelination after PNI

Nerve tissues were harvested 4 weeks post-operation and stained with the axon marker NF200 and the remyelination marker MBP to determine whether metformin treatment could promote axon regeneration and nerve remyelination. Nerve tissues from the metformin treatment group contained higher MBP and NF200 levels than the control group ($P < 0.05$, **Figure 2A-C**). Then, we retrogradely labeled with Dil to examine peripheral nerve regeneration, and there was a higher number of Dil-positive cells in the metformin treatment group than in the control group ($P < 0.01$, **Figure 1I** and **1J**). Altogether, these findings indicate that metformin treatment promotes axon regeneration

and remyelination of PNI in a crushing rat model.

Metformin promoted peripheral nerve regeneration by inducing M2 macrophage polarization

Our previous research showed that peripheral nerve regeneration is associated with M2 macrophage polarization [32] and that metformin exerts anti-inflammatory effects and possesses immunomodulatory properties. Therefore, we hypothesized that metformin could accelerate M2 macrophage polarization after PNI; to test this we performed immunofluorescence staining on the impaired nerve at 7 d post-operation. We used antibodies to CD68 as a marker for macrophages and used antibodies to CD206 as a marker for M2 macrophages. The number of CD68⁺CD206⁺ cells was higher in the metformin treatment group than in the control group ($P < 0.01$, **Figure 2D** and **2E**) indicating that metformin-induced M2 macrophage polarization.

Metformin converted inflammatory macrophage cells to M2 macrophage cells in vitro

To further demonstrate the effect of metformin on macrophage polarization, we asked whether metformin could accelerate M2 macrophage polarization *in vitro*. We extracted and purified BMDMs from mice as described previously [13] and treated them with 100 ng/ml LPS for 6 h to establish an *in vitro* inflammatory model of macrophages. To determine the optimal concentration of metformin to treat BMDMs, we used the CCK-8 assay to assess cell viability in the presence of various concentrations of metformin. BMDMs were seeded in 96-well plates and treated with 0.5, 1, 2, 4, 8, and 16 mmol/L metformin for 24 and 48 h. Because BMDMs treated with 2 mmol/L metformin yielded optimal cell viability ($P < 0.01$, **Figure 3A** and **3B**), 2 mmol/L of metformin was used in subsequent macrophage experiments. After treatment, the macrophage subpopulations were analyzed by flow cytometry. CD86⁺ F4/80⁺ was defined as the M1 macrophages and CD206⁺ F4/80⁺ was defined as the M2 macrophage. The distribution and density of M1 macrophages decreased in the metformin group compared to the control group ($P < 0.01$, **Figure 3C** and **3D**), and the distribution and density of M2 macrophages increased in the metformin group compared to the control group ($P < 0.01$, **Figure 3E** and **3F**).

Metformin in nerve regeneration

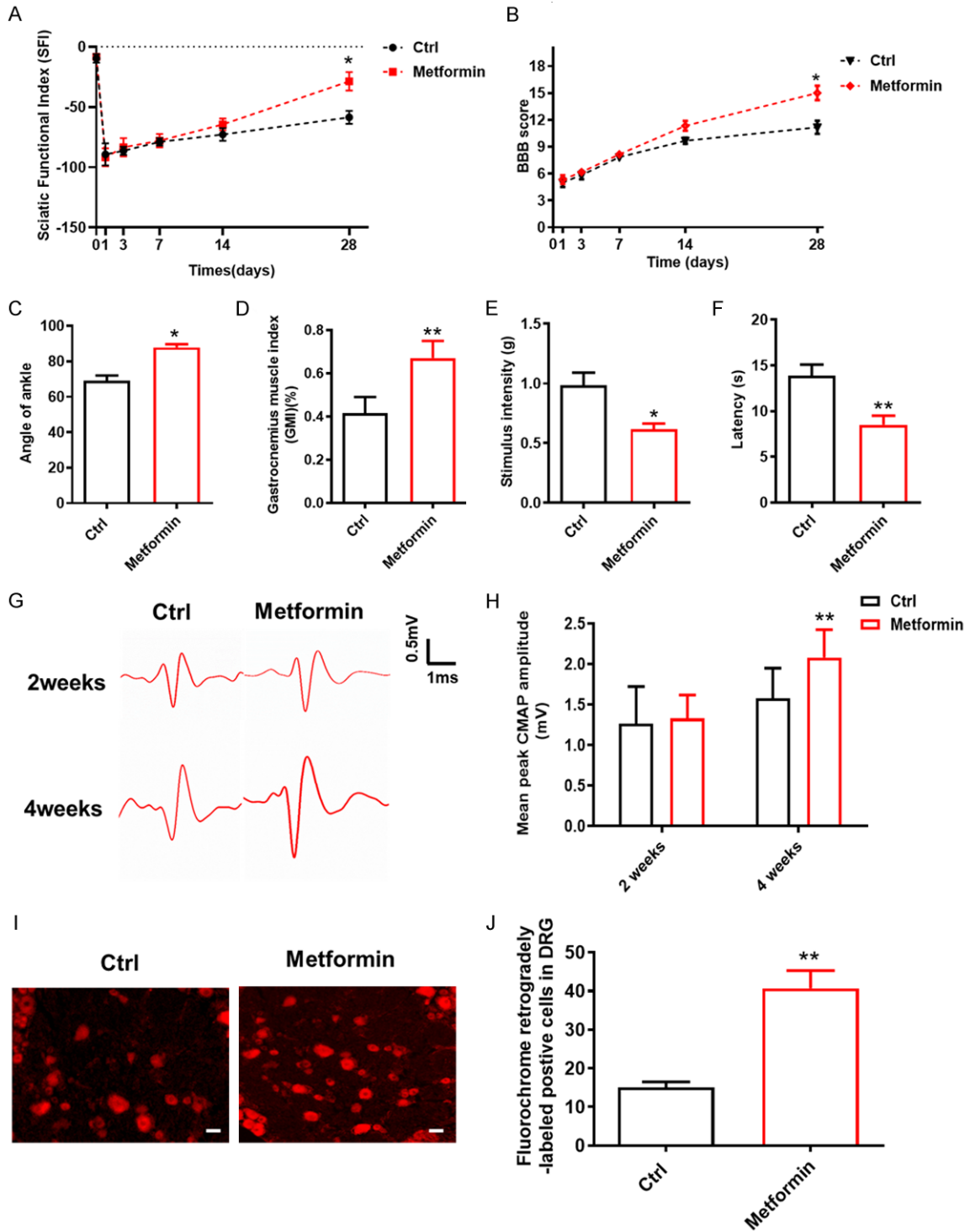


Figure 1. Metformin treatment improved functional recovery after peripheral nerve injury. A, B. Sciatic functional index (SFI) and Basso, Beattie, and Bresnahan (BBB) scores during functional motor recovery after sciatic nerve injury. C. Ankle angles at 4 weeks post-operation. D. The gastrocnemius muscle index (GMI) was used to evaluate the degree of muscle atrophy. E. Chemosensitivity analysis. F. Von-Frey test for functional sensory recovery at 4 weeks post-operation. G. Electrophysiology recordings at 2 weeks and 4 weeks post-operation. H. Quantitative electrophysiology data for compound motor action potential (CMAP) at 2 and 4 weeks post-operation. I. Retrograde labeling with Dil in dorsal root ganglia (DRG) at 4 weeks post-operation (original magnification $\times 200$). Scale bars are 25 μm . J. Quantitative analysis of retrograde labeling with Dil in DRG. Data are presented as mean \pm SD, $n = 6$, * $P < 0.05$, ** $P < 0.01$.

Metformin in nerve regeneration

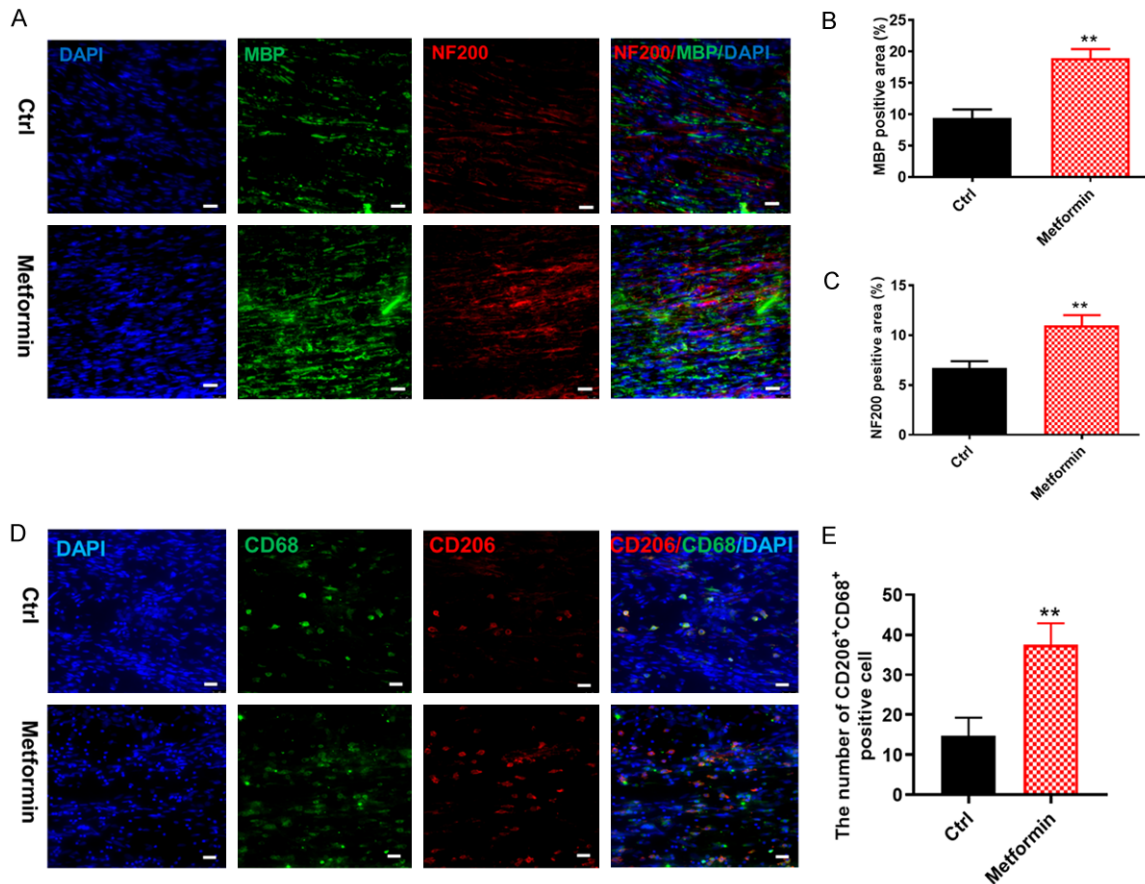


Figure 2. Immunofluorescence staining of neural tissue showed that metformin promoted axon regeneration and remyelination and accelerated M2 macrophage polarization after peripheral nerve injury. A. At 4 weeks post-operation, immunofluorescence staining with anti-neurofilament-200 (NF-200, red) was used to evaluate axon regeneration and immunofluorescence staining with anti-myelin basic protein (MBP, green) was used to evaluate remyelination. Tissues were counterstained with DAPI to mark the nuclei (blue) (original magnification $\times 200$). Scale bars are 25 μm . B, C. Quantitation of NF200 and MBP signals in the metformin and control groups. D. Immunofluorescence staining revealed different subpopulations of macrophages. CD68-positive (green) and CD206-positive (red) cells were defined as M2 macrophages (original magnification $\times 400$). Scale bars are 25 μm . E. Quantification of CD68⁺CD206⁺ cells. Data are presented as mean \pm SD, $n = 6$, * $P < 0.05$, ** $P < 0.01$.

We also measured expression of the M1 macrophage markers iNOS, TNF- α , and IL-1 β and expression of the M2 macrophage markers Arg-1, IL10, and Ym-1 by RT-qPCR. The relative mRNA expression of the M1 macrophage markers decreased in the metformin group compared to the control group (iNOS: $P < 0.05$, TNF- α : $P < 0.01$, IL-1 β : $P < 0.01$, **Figure 4A-C**). By contrast, the relative mRNA expression of the M2 macrophage markers increased in the metformin group compared to the control group (Arg-1: $P < 0.01$, IL10: $P < 0.01$, Ym-1: $P < 0.01$, **Figure 4D-F**). Altogether, these data demonstrate that metformin alleviates the LPS-induced inflammatory response and converts inflammatory macrophage cells to M2 macrophages.

Metformin converted inflammatory macrophage cells to M2 macrophage cells by modulating the AMPK/PGC-1 α /PPAR- γ signaling pathway

Next, we asked whether metformin could accelerate M2 macrophage polarization via the AMPK/PGC-1 α /PPAR- γ signaling. The expression levels of p-AMPK, AMPK, PGC- α , and PPAR- γ in BMDMs treated with and without metformin and/or compound C, an inhibitor of AMPK, were measured by Western blot (**Figure 5**). The p-AMPK/AMPK ratio was higher in the metformin group than in the control group ($P < 0.05$, **Figure 5B**). The expression levels of PGC- α and PPAR- γ were also higher in the metformin group than in the control group ($P <$

Metformin in nerve regeneration

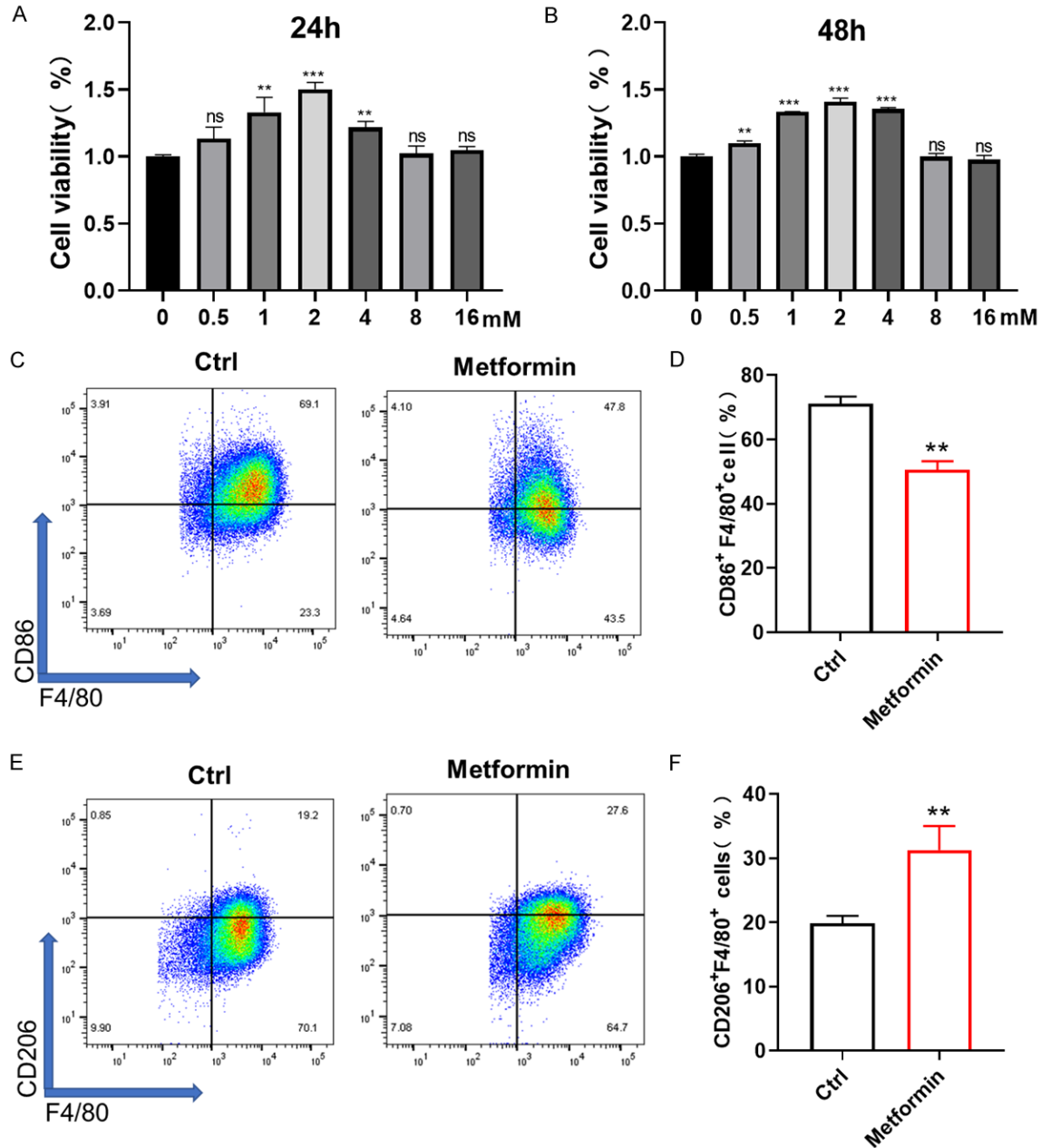


Figure 3. Metformin treatment accelerated M2 macrophage polarization *in vitro*. A, B. Cell viability of BMDMs upon treatment with various concentrations of metformin was evaluated by CCK-8 assay. C, E. Flow cytometry was used to detect surface markers on bone-marrow-derived macrophages. F4/80 was used as the pan-macrophage marker. CD86 was used as the M1 marker and CD206 was used as the M2 marker. D, F. Quantification of M1 and M2 macrophages in the metformin and control groups. Data are presented as mean \pm SD, $n = 3$, * $P < 0.05$, ** $P < 0.01$.

0.01, **Figure 5C** and **5D**). By contrast, when co-treated with metformin and compound C, the p-AMPK/AMPK ratio and the expression levels of PGC- α and PPAR- γ decreased to control levels (**Figure 5B-D**, $P < 0.01$) indicating that metformin activates PGC-1 α /PPAR- γ signaling by activating AMPK. Moreover, inhibition of AMPK

activity by compound C reversed the regulatory function of metformin. The distribution and density of M1 macrophages increased in the metformin + compound C group compared to the metformin group ($P < 0.01$, **Figure 6A** and **6B**), and the distribution and density of M2 macrophages were decreased in the metformin

Metformin in nerve regeneration

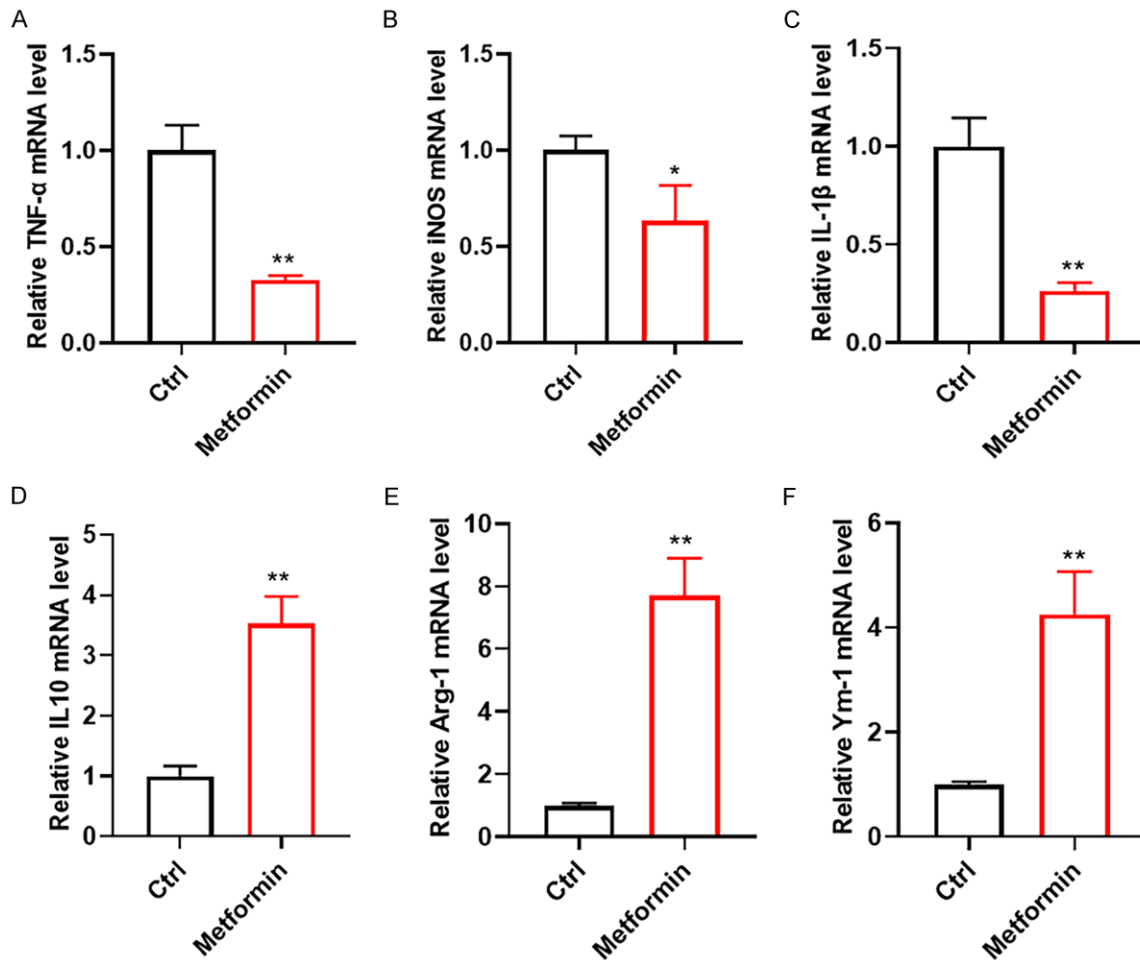


Figure 4. mRNA expression in M1 and M2 macrophages. A-C. The relative mRNA expression levels of inducible nitric oxide synthase (iNOS), tumor necrosis factor (TNF)- α , and interleukin (IL)-1 β (markers of M1 macrophages) were lower in the metformin treatment group than in the control group. D-F. The relative mRNA expression levels of arginase (Arg)-1, IL10, and chitinase 3-like 3 (Ym-1) (markers of M2 macrophages) were higher in the metformin treatment group than in the control group. Relative mRNA expression was measured by qPCR. Data are presented as mean \pm SD, n = 3, * P < 0.05, ** P < 0.01.

+ compound C group compared to the metformin group (P < 0.01, **Figure 6C** and **6D**). Altogether, these data showed that metformin regulates macrophage polarization and facilitates macrophage differentiation to M2 by regulating the AMPK/PGC-1 α /PPAR- γ signaling pathway.

Discussion

Metformin is a synthetic derivative of guanidine, an extract from the plant *Galega officinalis*, and is used worldwide for the treatment of type 2 diabetes [36, 37]. Recently, it has been demonstrated that metformin inhibits expression of pro-inflammatory cytokines, protects

against oxidative damage, and directs macrophage polarization [38, 39]. In addition, metformin was shown to inhibit inflammation and promote tissue repair by promoting M2 macrophage differentiation [8, 40]. Furthermore, M2 macrophages were shown to play a crucial role in peripheral nerve regeneration after injury [5, 41, 42]. However, the associations between metformin, M2 macrophage polarization, and peripheral nerve regeneration remain unknown. Therefore, the objective of this study was to determine whether metformin could switch macrophages to the M2 subtype to increase peripheral nerve regeneration. Our results demonstrated that metformin administration induced significant regeneration in the PNI

Metformin in nerve regeneration

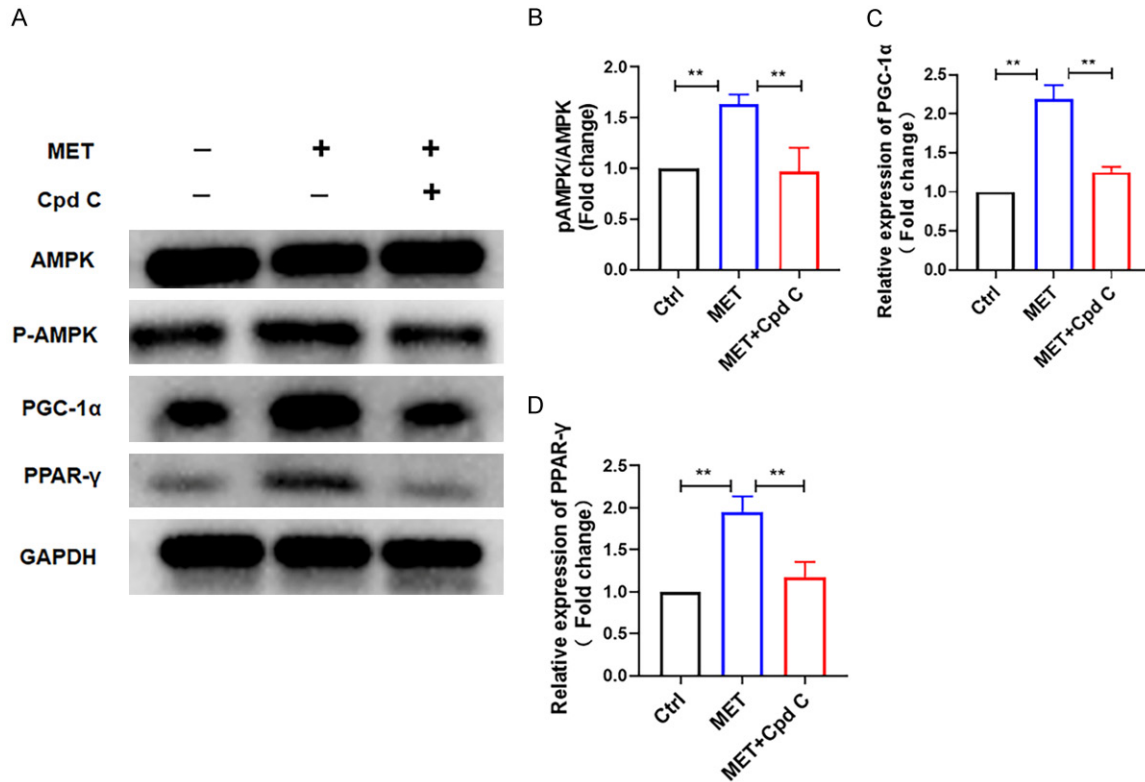


Figure 5. Metformin-induced M2 macrophage polarization via the AMPK/PGC-1 α /PPAR- γ signaling pathway. A. Protein expression levels of AMP-activated protein kinase (AMPK), phosphorylated (p)-AMPK, proliferator-activated receptor- γ co-activator 1 α (PGC-1 α), peroxisome proliferator-activated receptor- γ (PPAR- γ), and GAPDH were evaluated by Western blot. B. The quantified p-AMPK/AMPK ratio is a measure of AMPK activation. C, D. Quantification of relative expression of PGC-1 α and PPAR- γ . Abbreviations: MET, metformin; Cpd C, Compound C. Data are presented as mean \pm SD, n = 3, **P < 0.01.

model as observed by improved recovery of motor and sensory functions and increased axon regeneration and myelination. In addition, we observed metformin-induced M2 macrophage polarization *in vivo*. *In vitro*, we demonstrated that metformin promotes M2 macrophage polarization via the AMPK/PGC-1 α /PPAR- γ signaling pathway.

Earlier studies extensively addressed the neuroprotective effects of metformin and revealed its positive therapeutic effects in animal models of spinal cord injury (SCI) [43], PNI [44], and cerebral ischemia [45]. Mary *et al.* found that metformin regulates autophagy by reducing reactive oxygen species production and mitigates peripheral nerve damage in non-obese diabetic mice (MKR) [46]. Wang *et al.* found that metformin stabilizes microtubule structure, regulates oxidative stress and mitochondria function by activating the Akt-mediated Nrf2/ARE pathway, and promotes axonal regen-

eration after SCI [47]. However, few studies focused on the immunomodulatory ability, specifically macrophage reprogramming, of metformin during peripheral nerve regeneration. Therefore, our findings that metformin enhances functional recovery in an animal model of PNI by regulating M2 macrophage polarization are novel.

It is well known that peripheral nerve regeneration requires the participation of macrophages. Induction of M2 macrophage polarization can accelerate regeneration of axons and myelin sheaths [48]. Emerging research illustrated that M2 macrophages could release vascular endothelial growth factor to induce vascular regeneration at the site of peripheral nerve damage, which is critical for nerve regeneration [49]. It was also shown that M2 macrophages could promote Schwann cell maturity [5, 50]. These findings provide strong evidence for the essential role of M2 macrophages in the periph-

Metformin in nerve regeneration

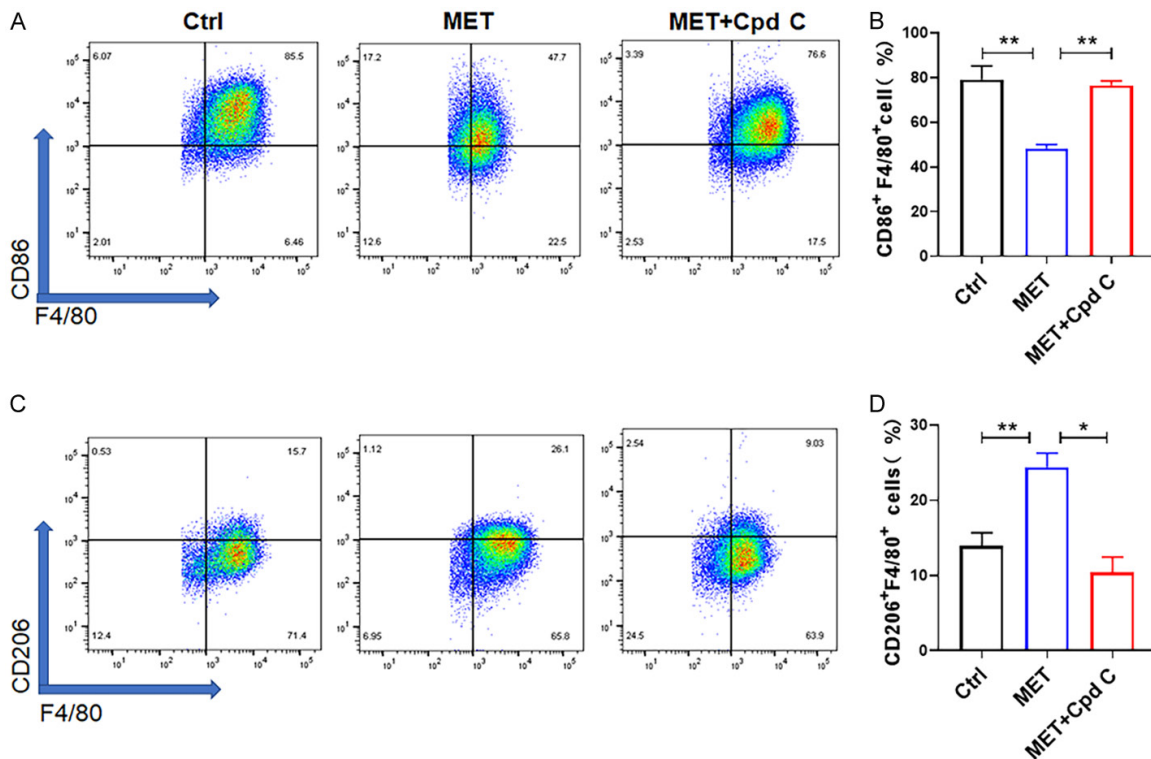


Figure 6. Inhibition of AMP-activated protein kinase activity by compound C reversed the regulatory function of metformin *in vitro*. A, C. Flow cytometry detection of surface markers on bone-marrow-derived macrophages. F4/80 was used as the pan-macrophage marker. CD86 was used as the M1 macrophage marker and CD206 was used as the M2 macrophage marker. B, D. Quantification of the proportion of M1 and M2 macrophages. Abbreviations: MET, metformin; Cpd C, Compound C. Data are presented as mean \pm SD, $n = 3$, * $P < 0.05$, ** $P < 0.01$.

eral nerve regeneration process and suggest that targeting macrophages may be a promising strategy to improve functional recovery outcomes after PNI. In this study, metformin was shown to upregulate the number and proportion of M2 macrophages. *In vitro*, pre-treatment with LPS stimulated polarization of the primary macrophage to the M1 phenotype, which mimics activation of inflammation in the early stages of nerve injury. Metformin treatment reversed the pro-inflammatory effect of LPS and upregulated expression of the M2 macrophage marker CD206, but this effect of metformin was reversed with the addition of compound C, an AMPK inhibitor. These results indicate that metformin promotes the regeneration of axons and myelin sheaths through polarization of macrophages to the M2 type and activation of AMPK.

Macrophage polarization was found to be involved in the regulation of energy metabolism [51, 52]. AMPK, the target of metformin, is essential for cellular metabolism and growth.

Previous studies showed that activated AMPK is involved in tissue repair resulting from multiple pathological processes, including ulcerative colitis [53], rheumatoid arthritis [54], and diabetic ulcers [55]. In the field of nerve regeneration, the positive effects of AMPK have been confirmed by numerous studies. It has been shown that AMPK regulates mitochondrial autophagy and remodeling in neurons and is involved in nerve growth factor (NGF)-induced neuronal differentiation [56]. In addition, Li et al. have demonstrated that NGF enhanced the ability of Schwann cells to phagocytose and clear degenerated myelin by activating the AMPK/mTOR pathway and promoted the recovery after PNI [16]. The role of energy metabolism and mitochondrial homeostasis in nerve regeneration has been increasingly demonstrated [57-59]. Furthermore, AMPK can promote mitochondrial biogenesis and homeostasis by activating PGC-1 α /PPAR- γ signaling pathway [60, 61]. Numerous studies have shown that the AMPK pathway is critical in the regulation of inflammation and tissue regenera-

tion. Ma *et al.* confirmed that SIRT1 could stimulate oxidative energy production by activating AMPK, PPAR- γ , and PGC-1 α simultaneously, and these factors were found to suppress NF- κ B signaling and inflammation. It was also argued that inhibition of the AMPK/PGC-1 α /PPAR- γ signaling pathway could induce chronic inflammation associated with metabolic diseases. Yang *et al.* have proved that Magnolol effectively ameliorates diabetic peripheral neuropathy in mice via activating AMPK/PGC-1 α /PPAR- γ signaling pathway [62]. In addition, there is research suggesting that FGF21 regulates AMPK/PGC-1 α /PPAR- γ signaling pathway and attenuates hypoxia-induced pulmonary hypertension [63]. Thus, we hypothesized that the regulatory function of metformin is associated with the AMPK/PGC-1 α /PPAR- γ signaling pathway. Western blotting was applied to clarify the molecular mechanism of metformin-induced M2 macrophage polarization during nerve regeneration process. The results show that metformin significantly elevated the p-AMPK/AMPK ratio, as well as the expression levels of PGC- α and PPAR- γ . By contrast, the p-AMPK/AMPK ratio and PGC- α and PPAR- γ expression levels in cells co-treated with metformin and compound C decreased indicating that metformin activates PGC-1 α /PPAR- γ signaling by activating AMPK. Moreover, we observed that inhibition of AMPK activity by compound C reversed the regulatory function of metformin. In this study, metformin treatment promoted alternative M2 macrophage polarization by activating AMPK, which upregulates the PGC-1 α /PPAR- γ signaling pathway. Therefore, we suggest that the effect of metformin on wound healing may be due to regulation of the AMPK/PGC-1 α /PPAR- γ signaling axis leading to alteration of the macrophage phenotype. Notably, our findings revealed a novel molecular mechanism in which metformin enhances functional recovery in an animal model of PNI by regulating M2 macrophage polarization. Our results suggest that metformin is a promising therapeutic strategy to modulate the AMPK/PGC-1 α /PPAR- γ signaling pathway and induce M2 macrophage polarization.

Acknowledgements

We would like to thank the Institute of Medical Science, Xiangya Hospital of the Central South University for invaluable assistance in conduct-

ing these experiments, and the other members of the research group for useful discussion in preparing this manuscript.

Disclosure of conflict of interest

The authors declare that the research was conducted in the absence of any commercial or financial relationships that could be construed as a potential conflict of interest.

Address correspondence to: Liming Qing and Juyu Tang, Department of Orthopedics, Hand and Microsurgery, Xiangya Hospital of Central South University, No. 87 Xiangya Road, Changsha 410008, Hunan, China. E-mail: qingliming@csu.edu.cn (LMQ); tangjuyu@csu.edu.cn (JYT)

References

- [1] Lopes B, Sousa P, Alvites R, Branquinho M, Sousa AC, Mendonça C, Atayde LM, Luís AL, Varejão ASP and Maurício AC. Peripheral nerve injury treatments and advances: one health perspective. *Int J Mol Sci* 2022; 23: 918.
- [2] Sun JX, Xu XH and Jin L. Effects of metabolism on macrophage polarization under different disease backgrounds. *Front Immunol* 2022; 13: 880286.
- [3] Tang D, Cao F, Yan C, Fang K, Ma J, Gao L, Sun B and Wang G. Extracellular vesicle/macrophage axis: potential targets for inflammatory disease intervention. *Front Immunol* 2022; 13: 705472.
- [4] Liu P, Peng J, Han GH, Ding X, Wei S, Gao G, Huang K, Chang F and Wang Y. Role of macrophages in peripheral nerve injury and repair. *Neural Regen Res* 2019; 14: 1335-1342.
- [5] Li J, Yao Y, Wang Y, Xu J, Zhao D, Liu M, Shi S and Lin Y. Modulation of the crosstalk between Schwann cells and macrophages for nerve regeneration: a therapeutic strategy based on a multifunctional tetrahedral framework nucleic acids system. *Adv Mater* 2022; 34: e2202513.
- [6] Matsui Y, Kadoya K, Nagano Y, Endo T, Hara M, Matsumae G, Suzuki T, Yamamoto Y, Terkawi MA and Iwasaki N. IL4 stimulated macrophages promote axon regeneration after peripheral nerve injury by secreting uPA to stimulate uPAR upregulated in injured axons. *Cell Mol Life Sci* 2022; 79: 289.
- [7] Kotwal GJ and Chien S. Macrophage differentiation in normal and accelerated wound healing. *Results Probl Cell Differ* 2017; 62: 353-364.
- [8] Liu H, Duan C, Yang X, Liu J, Deng Y, Tiselius HG, Ye Z, Wang T, Xing J and Xu H. Metformin suppresses calcium oxalate crystal-induced kidney injury by promoting Sirt1 and M2 mac-

Metformin in nerve regeneration

- rophage-mediated anti-inflammatory activation. *Signal Transduct Target Ther* 2023; 8: 38.
- [9] Liu J, Lu J, Zhang L, Liu Y, Zhang Y, Gao Y, Yuan X, Xiang M and Tang Q. The combination of exercise and metformin inhibits TGF- β 1/Smad pathway to attenuate myocardial fibrosis in db/db mice by reducing NF- κ B-mediated inflammatory response. *Biomed Pharmacother* 2023; 157: 114080.
- [10] Zhang C, Huang H, Chen J, Zuo T, Ou Q, Ruan G, He J and Ding C. DNA supramolecular hydrogel-enabled sustained delivery of metformin for relieving osteoarthritis. *ACS Appl Mater Interfaces* 2023; 15: 16369-16379.
- [11] Chen GG, Woo PYM, Ng SCP, Wong GKC, Chan DTM, van Hasselt CA, Tong MCF and Poon WS. Impact of metformin on immunological markers: implication in its anti-tumor mechanism. *Pharmacol Ther* 2020; 213: 107585.
- [12] Ma R, Yi B, Riker AI and Xi Y. Metformin and cancer immunity. *Acta Pharmacol Sin* 2020; 41: 1403-1409.
- [13] Qing L, Fu J, Wu P, Zhou Z, Yu F and Tang J. Metformin induces the M2 macrophage polarization to accelerate the wound healing via regulating AMPK/mTOR/NLRP3 inflammatory signaling pathway. *Am J Transl Res* 2019; 11: 655-668.
- [14] Foretz M, Guigas B and Viollet B. Understanding the glucoregulatory mechanisms of metformin in type 2 diabetes mellitus. *Nat Rev Endocrinol* 2019; 15: 569-589.
- [15] LaMoia TE and Shulman GI. Cellular and molecular mechanisms of metformin action. *Endocr Rev* 2021; 42: 77-96.
- [16] Li R, Li D, Wu C, Ye L, Wu Y, Yuan Y, Yang S, Xie L, Mao Y, Jiang T, Li Y, Wang J, Zhang H, Li X and Xiao J. Nerve growth factor activates autophagy in Schwann cells to enhance myelin debris clearance and to expedite nerve regeneration. *Theranostics* 2020; 10: 1649-1677.
- [17] Xia W, Zhu J, Wang X, Tang Y, Zhou P, Hou M and Li S. ANXA1 directs Schwann cells proliferation and migration to accelerate nerve regeneration through the FPR2/AMPK pathway. *FASEB J* 2020; 34: 13993-14005.
- [18] Ma T, Hao Y, Li S, Xia B, Gao X, Zheng Y, Mei L, Wei Y, Yang C, Lu L, Luo Z and Huang J. Sequential oxygen supply system promotes peripheral nerve regeneration by enhancing Schwann cells survival and angiogenesis. *Biomaterials* 2022; 289: 121755.
- [19] Zhu J, Wang KZ and Chu CT. After the banquet: mitochondrial biogenesis, mitophagy, and cell survival. *Autophagy* 2013; 9: 1663-1676.
- [20] Islam H, Edgett BA and Gurd BJ. Coordination of mitochondrial biogenesis by PGC-1 α in human skeletal muscle: a re-evaluation. *Metabolism* 2018; 79: 42-51.
- [21] Corona JC and Duchon MR. PPAR γ and PGC-1 α as therapeutic targets in Parkinson's. *Neurochem Res* 2015; 40: 308-316.
- [22] Nijland PG, Witte ME, van het Hof B, van der Pol S, Bauer J, Lassmann H, van der Valk P, de Vries HE and van Horsen J. Astroglial PGC-1 α increases mitochondrial antioxidant capacity and suppresses inflammation: implications for multiple sclerosis. *Acta Neuropathol Commun* 2014; 2: 170.
- [23] Rosenkranz SC, Shaposhnykov AA, Träger S, Engler JB, Witte ME, Roth V, Vieira V, Paauw N, Bauer S, Schwencke-Westphal C, Schubert C, Bal LC, Schattling B, Pless O, van Horsen J, Freichel M and Friese MA. Enhancing mitochondrial activity in neurons protects against neurodegeneration in a mouse model of multiple sclerosis. *Elife* 2021; 10: e61798.
- [24] Pasquinelli A, Chico L, Pasquali L, Bisordi C, Lo Gerfo A, Fabbrini M, Petrozzi L, Marconi L, Caldarazzo Ienco E, Mancuso M and Siciliano G. Gly482Ser PGC-1 α gene polymorphism and exercise-related oxidative stress in amyotrophic lateral sclerosis patients. *Front Cell Neurosci* 2016; 10: 102.
- [25] Varghese M, Zhao W, Trageser KJ and Pasinetti GM. Peroxisome proliferator activator receptor gamma coactivator-1 α overexpression in amyotrophic lateral sclerosis: a tale of two transgenics. *Biomolecules* 2020; 10: 760.
- [26] Wang R, Li JJ, Diao S, Kwak YD, Liu L, Zhi L, Büeler H, Bhat NR, Williams RW, Park EA and Liao FF. Metabolic stress modulates Alzheimer's β -secretase gene transcription via SIRT1-PPAR γ -PGC-1 in neurons. *Cell Metab* 2013; 17: 685-694.
- [27] Katsouri L, Lim YM, Blodrath K, Eleftheriadou I, Lombardero L, Birch AM, Mirzaei N, Irvine EE, Mazarakis ND and Sastre M. PPAR γ -coactivator-1 α gene transfer reduces neuronal loss and amyloid- β generation by reducing β -secretase in an Alzheimer's disease model. *Proc Natl Acad Sci U S A* 2016; 113: 12292-12297.
- [28] Zhong J, Dong W, Qin Y, Xie J, Xiao J, Xu J and Wang H. Roflupram exerts neuroprotection via activation of CREB/PGC-1 α signalling in experimental models of Parkinson's disease. *Br J Pharmacol* 2020; 177: 2333-2350.
- [29] Jo A, Lee Y, Kam TI, Kang SU, Neifert S, Karuppagounder SS, Khang R, Kang H, Park H, Chou SC, Oh S, Jiang H, Swing DA, Ham S, Pirooznia S, Umanah GKE, Mao X, Kumar M, Ko HS, Kang HC, Lee BD, Lee YI, Andrabi SA, Park CH, Lee JY, Kim H, Kim H, Kim H, Cho JW, Paek SH, Na CH, Tessarollo L, Dawson VL, Dawson TM and Shin JH. PARIS farnesylation prevents neurodegeneration in models of Parkinson's disease. *Sci Transl Med* 2021; 13: eaax8891.

- [30] Ma CH, Chiua YC, Wu CH, Jou IM, Tu YK, Hung CH, Hsieh PL and Tsai KL. Homocysteine causes dysfunction of chondrocytes and oxidative stress through repression of SIRT1/AMPK pathway: a possible link between hyperhomocysteinemia and osteoarthritis. *Redox Biol* 2018; 15: 504-512.
- [31] Li L, Chen X, Su C, Wang Q, Li R, Jiao W, Luo H, Tian Y, Tang J, Li X, Liu B, Wang W, Zhang D and Guo S. Si-Miao-Yong-An decoction preserves cardiac function and regulates GLC/AMPK/NF- κ B and GLC/PPAR α /PGC-1 α pathways in diabetic mice. *Biomed Pharmacother* 2020; 132: 110817.
- [32] Li C, Li X, Shi Z, Wu P, Fu J, Tang J and Qing L. Exosomes from LPS-preconditioned bone marrow MSCs accelerated peripheral nerve regeneration via M2 macrophage polarization: involvement of TSG-6/NF-kappaB/NLRP3 signaling pathway. *Exp Neurol* 2022; 356: 114139.
- [33] Dinh P, Hazel A, Palispis W, Suryadevara S and Gupta R. Functional assessment after sciatic nerve injury in a rat model. *Microsurgery* 2009; 29: 644-649.
- [34] Bain JR, Mackinnon SE and Hunter DA. Functional evaluation of complete sciatic, peroneal, and posterior tibial nerve lesions in the rat. *Plast Reconstr Surg* 1989; 83: 129-138.
- [35] Ying W, Cheruku PS, Bazer FW, Safe SH and Zhou B. Investigation of macrophage polarization using bone marrow derived macrophages. *J Vis Exp* 2013; 50323.
- [36] Triggler CR, Mohammed I, Bshesh K, Marei I, Ye K, Ding H, MacDonald R, Hollenberg MD and Hill MA. Metformin: is it a drug for all reasons and diseases? *Metabolism* 2022; 133: 155223.
- [37] Khan J, Pernicova I, Nisar K and Korbonits M. Mechanisms of ageing: growth hormone, dietary restriction, and metformin. *Lancet Diabetes Endocrinol* 2023; 11: 261-281.
- [38] Scheen AJ, Esser N and Paquot N. Antidiabetic agents: potential anti-inflammatory activity beyond glucose control. *Diabetes Metab* 2015; 41: 183-194.
- [39] Ahmadi A, Panahi Y, Johnston TP and Sahebkar A. Antidiabetic drugs and oxidized low-density lipoprotein: a review of anti-atherosclerotic mechanisms. *Pharmacol Res* 2021; 172: 105819.
- [40] Yuan D, Li Y, Hou L, Yang F, Meng C, Yu Y, Sun C, Duan G, Xu Z, Zhu G, Guo J, Zhang L, Yan G, Chen J, Yang Y, Zhang Y and Gao Y. Metformin regulates alveolar macrophage polarization to protect against acute lung injury in rats caused by paraquat poisoning. *Front Pharmacol* 2022; 13: 811372.
- [41] Liu D, Lu G, Shi B, Ni H, Wang J, Qiu Y, Yang L, Zhu Z, Yi X, Du X and Shi B. ROS-scavenging hydrogels synergize with neural stem cells to enhance spinal cord injury repair via regulating microenvironment and facilitating nerve regeneration. *Adv Healthc Mater* 2023; e2300123.
- [42] Yang Q, Su S, Liu S, Yang S, Xu J, Zhong Y, Yang Y, Tian L, Tan Z, Wang J, Yu Z, Shi Z and Liang F. Exosomes-loaded electroconductive nerve dressing for nerve regeneration and pain relief against diabetic peripheral nerve injury. *Bioact Mater* 2023; 26: 194-215.
- [43] Chen Q, Xie D, Yao Q and Yang L. Effect of metformin on locomotor function recovery in rat spinal cord injury model: a meta-analysis. *Oxid Med Cell Longev* 2021; 2021: 1948003.
- [44] Ma J, Liu J, Yu H, Chen Y, Wang Q and Xiang L. Beneficial effect of metformin on nerve regeneration and functional recovery after sciatic nerve crush injury in diabetic rats. *Neurochem Res* 2016; 41: 1130-1137.
- [45] Leech T, Chattipakorn N and Chattipakorn SC. The beneficial roles of metformin on the brain with cerebral ischaemia/reperfusion injury. *Pharmacol Res* 2019; 146: 104261.
- [46] Haddad M, Eid S, Harb F, Massry MEL, Azar S, Sauleau EA and Eid AA. Activation of 20-HETE synthase triggers oxidative injury and peripheral nerve damage in type 2 diabetic mice. *J Pain* 2022; 23: 1371-1388.
- [47] Wang H, Zheng Z, Han W, Yuan Y, Li Y, Zhou K, Wang Q, Xie L, Xu K, Zhang H, Xu H, Wu Y and Xiao J. Metformin promotes axon regeneration after spinal cord injury through inhibiting oxidative stress and stabilizing microtubule. *Oxid Med Cell Longev* 2020; 2020: 9741369.
- [48] Zigmund RE and Echevarria FD. Macrophage biology in the peripheral nervous system after injury. *Prog Neurobiol* 2019; 173: 102-121.
- [49] Bartus K, James ND, Didangelos A, Bosch KD, Verhaagen J, Yáñez-Muñoz RJ, Rogers JH, Schneider BL, Muir EM and Bradbury EJ. Large-scale chondroitin sulfate proteoglycan digestion with chondroitinase gene therapy leads to reduced pathology and modulates macrophage phenotype following spinal cord contusion injury. *J Neurosci* 2014; 34: 4822-4836.
- [50] Zhang Q, Burrell JC, Zeng J, Motiwala FI, Shi S, Cullen DK and Le AD. Implantation of a nerve protector embedded with human GMSC-derived Schwann-like cells accelerates regeneration of crush-injured rat sciatic nerves. *Stem Cell Res Ther* 2022; 13: 263.
- [51] Ren W, Xia Y, Chen S, Wu G, Bazer FW, Zhou B, Tan B, Zhu G, Deng J and Yin Y. Glutamine metabolism in macrophages: a novel target for obesity/type 2 diabetes. *Adv Nutr* 2019; 10: 321-330.
- [52] Kapralov AA, Yang Q, Dar HH, Tyurina YY, Anthonymuthu TS, Kim R, St Croix CM, Mikulska-Ruminska K, Liu B, Shrivastava IH, Tyurin VA,

Metformin in nerve regeneration

- Ting HC, Wu YL, Gao Y, Shurin GV, Artyukhova MA, Ponomareva LA, Timashev PS, Domingues RM, Stoyanovsky DA, Greenberger JS, Mallampalli RK, Bahar I, Gabrilovich DI, Bayır H and Kagan VE. Redox lipid reprogramming commands susceptibility of macrophages and microglia to ferroptotic death. *Nat Chem Biol* 2020; 16: 278-290.
- [53] Xu X, Wang Y, Wei Z, Wei W, Zhao P, Tong B, Xia Y and Dai Y. Madecassic acid, the contributor to the anti-colitis effect of madecassoside, enhances the shift of Th17 toward Treg cells via the PPAR γ /AMPK/ACC1 pathway. *Cell Death Dis* 2017; 8: e2723.
- [54] Seoane-Collazo P, Rial-Pensado E, Estévez-Salguero Á, Milbank E, García-Caballero L, Ríos M, Liñares-Pose L, Scotecce M, Gallego R, Fernández-Real JM, Nogueiras R, Diéguez C, Gualillo O and López M. Activation of hypothalamic AMP-activated protein kinase ameliorates metabolic complications of experimental arthritis. *Arthritis Rheumatol* 2022; 74: 212-222.
- [55] Lin JT, Chen HM, Chiu CH and Liang YJ. AMP-activated protein kinase activators in diabetic ulcers: from animal studies to phase II drugs under investigation. *Expert Opin Investig Drugs* 2014; 23: 1253-1265.
- [56] Martorana F, Gaglio D, Bianco MR, Aprea F, Virtuoso A, Bonanomi M, Alberghina L, Papa M and Colangelo AM. Differentiation by nerve growth factor (NGF) involves mechanisms of crosstalk between energy homeostasis and mitochondrial remodeling. *Cell Death Dis* 2018; 9: 391.
- [57] Shefa U, Jeong NY, Song IO, Chung HJ, Kim D, Jung J and Huh Y. Mitophagy links oxidative stress conditions and neurodegenerative diseases. *Neural Regen Res* 2019; 14: 749-756.
- [58] Ineichen BV, Zhu K and Carlström KE. Axonal mitochondria adjust in size depending on g-ratio of surrounding myelin during homeostasis and advanced remyelination. *J Neurosci Res* 2021; 99: 793-805.
- [59] Han L, Dong X, Qiu T, Dou Z, Wu L and Dai H. Enhanced sciatic nerve regeneration by relieving iron-overloading and organelle stress with the nanofibrous P(MMD-co-LA)/DFO conduits. *Mater Today Bio* 2022; 16: 100387.
- [60] Chamoto K, Chowdhury PS, Kumar A, Sonomura K, Matsuda F, Fagarasan S and Honjo T. Mitochondrial activation chemicals synergize with surface receptor PD-1 blockade for T cell-dependent antitumor activity. *Proc Natl Acad Sci U S A* 2017; 114: E761-E770.
- [61] Koh JH, Hancock CR, Terada S, Higashida K, Holloszy JO and Han DH. PPAR β is essential for maintaining normal levels of PGC-1 α and mitochondria and for the increase in muscle mitochondria induced by exercise. *Cell Metab* 2017; 25: 1176-1185, e5.
- [62] Yang J, Wei Y, Zhao T, Li X, Zhao X, Ouyang X, Zhou L, Zhan X, Qian M, Wang J and Shen X. Magnolol effectively ameliorates diabetic peripheral neuropathy in mice. *Phytomedicine* 2022; 107: 154434.
- [63] Cai G, Liu J, Wang M, Su L, Cai M, Huang K, Li X, Li M, Wang L and Huang X. Mutual promotion of FGF21 and PPAR γ attenuates hypoxia-induced pulmonary hypertension. *Exp Biol Med (Maywood)* 2019; 244: 252-261.